

# **Seasonal Dynamics of Epiphytic Microbial Communities on Marine Macrophyte Surfaces**

Marino Korlević<sup>1\*</sup>, Marsej Markovski<sup>1</sup>, Zihao Zhao<sup>2</sup>, Gerhard J. Herndl<sup>2,3</sup>, Mirjana Najdek<sup>1</sup>

1. Center for Marine Research, Ruđer Bošković Institute, Croatia

2. Department of Functional and Evolutionary Ecology, University of Vienna, Austria

3. NIOZ, Department of Marine Microbiology and Biogeochemistry, Royal Netherlands Institute for Sea Research, Utrecht University, The Netherlands

\*To whom correspondence should be addressed:

Marino Korlević

G. Paliaga 5, 52210 Rovinj, Croatia

Tel.: +385 52 804 768

Fax: +385 52 804 780

e-mail: [marino.korlevic@irb.hr](mailto:marino.korlevic@irb.hr)

Running title: Seasonal dynamics of epiphytic communities

## 1 Abstract

2 Surfaces of marine macrophytes are inhabited by diverse microbial communities. Most  
3 studies focusing on epiphytic communities of macrophytes did not take into account temporal  
4 changes or applied low sampling frequency approaches. The seasonal dynamics of epiphytic  
5 microbial communities was determined in a meadow of *Cymodocea nodosa* invaded by *Caulerpa*  
6 *cylindracea* and in a monospecific settlement of *Caulerpa cylindracea* at monthly intervals. For  
7 comparison the ambient prokaryotic picoplankton community was also characterized. At the OTU  
8 level, the microbial community composition differed between the ambient water and the epiphytic  
9 communities exhibiting host-specificity. Also, successional changes were observed connected to  
10 the macrophyte growth cycle. Taxonomic analysis, however, showed similar high rank groups in  
11 the ambient water and the epiphytic communities, with the exception of *Desulfobacterota*, which  
12 were only found on *Caulerpa cylindracea*. *Cyanobacteria* showed seasonal changes while other  
13 high rank taxa were present throughout the year. Phylogenetic groups present throughout the year  
14 constituted most of the sequences, while less abundant taxa showed seasonal patterns connected  
15 to the macrophyte growth cycle. Taken together, epiphytic microbial communities of the seagrass  
16 *Cymodocea nodosa* and the macroalga *Caulerpa cylindracea* appear to be host-specific and contain  
17 taxa that undergo successional changes.

18 **Introduction**

19       Marine macrophytes (seagrasses and macroalgae) are important ecosystem engineers forming  
20 close associations with microorganisms belonging to all three domains of life (Egan et al., 2013;  
21 Tarquinio et al., 2019). Microbes can live within macrophyte tissue as endophytes or can form  
22 epiphytic communities on surfaces of leaves and thalli (Egan et al., 2013; Hollants et al., 2013;  
23 Tarquinio et al., 2019). Epiphytic and endophytic microbial communities exhibit a close functional  
24 relationship with the macrophyte host. It was proposed that this close relationship constitutes a  
25 holobiont, an integrated community where the macrophyte organism and its symbiotic partners  
26 support each other (Margulis, 1991; Egan et al., 2013; Tarquinio et al., 2019).

27       Biofilms of microbial epiphytes can contain diverse taxonomic groups and harbor cell  
28 abundances from  $10^2$  to  $10^7$  cells  $\text{cm}^{-2}$  (Armstrong et al., 2000; Bengtsson et al., 2010; Burke et  
29 al., 2011b). In such an environment a number of positive and negative interactions between the  
30 macrophyte and the colonizing microorganisms have been described (Egan et al., 2013; Hollants  
31 et al., 2013; Tarquinio et al., 2019). Macrophytes can promote growth of associated microbes by  
32 nutrient exudation, while in return microorganisms may support macrophyte performance through  
33 improved nutrient availability, phytohormone production and protection from toxic compounds,  
34 oxidative stress, biofouling organisms and pathogens (Egan et al., 2013; Hollants et al., 2013;  
35 Tarquinio et al., 2019). Besides these positive interactions, macrophytes can negatively impact  
36 the associated microbes such as pathogenic bacteria by producing reactive oxygen species and  
37 secondary metabolites (Egan et al., 2013; Hollants et al., 2013; Tarquinio et al., 2019).

38       All these ecological roles are carried out by a taxonomically diverse community of  
39 microorganisms. At higher taxonomic ranks a core set of macrophyte epiphytic taxa was described  
40 consisting mainly of *Alphaproteobacteria*, *Gammaproteobacteria*, *Desulfobacterota*, *Bacteroidota*,  
41 *Cyanobacteria*, *Actinobacteriota*, *Firmicutes*, *Planctomycetota*, *Chloroflexi* and *Verrucomicrobiota*  
42 (Crump and Koch, 2008; Tujula et al., 2010; Lachnit et al., 2011). In contrast, at lower taxonomic

43 ranks host specific microbial communities were found (Lachnit et al., 2011; Roth-Schulze et  
44 al., 2016). Recently, it was shown that even different morphological niches within the same  
45 alga had a higher influence on the composition of the bacterial community than biogeography or  
46 environmental factors (Morrissey et al., 2019). While the microbial community composition varies  
47 between host species, metagenomic analyses revealed that the majority of the microbial functions  
48 are conserved (Burke et al., 2011a; Roth-Schulze et al., 2016). This discrepancy between the  
49 microbial taxonomic and functional composition might be explained by the lottery hypothesis. It  
50 postulates that an initial random colonization step takes places from a set of functionally equivalent  
51 taxonomic groups resulting in taxonomically different epiphytic communities sharing a core set of  
52 functional genes (Burke et al., 2011a; Roth-Schulze et al., 2016). In addition, some of the variation  
53 in the reported data could be attributed to different techniques used in these studies, such as different  
54 protocols for epiphytic cell detachment and/or DNA isolation, as no standard protocol has been yet  
55 established to study epiphytic communities (Ugarelli et al., 2019; Korlević et al., submitted).

56 The majority of studies describing macrophyte epiphytic microbial communities did not  
57 include possible seasonal changes (Crump and Koch, 2008; Lachnit et al., 2009; Burke et al., 2011b;  
58 Roth-Schulze et al., 2016; Ugarelli et al., 2019). If seasonal changes were taken into account, low  
59 temporal frequency, applied methodologies and/or limited number of analysed host species did not  
60 allow a high taxonomic resolution (Tujula et al., 2010; Lachnit et al., 2011; Michelou et al., 2013;  
61 Miranda et al., 2013; Mancuso et al., 2016). In the present study we describe the seasonal dynamics  
62 of bacterial and archaeal communities on the surfaces of the seagrass *Cymodocea nodosa* and  
63 siphonous macroalgae *Caulerpa cylindracea* determined on a mostly monthly scale. Bacterial and  
64 archaeal epiphytes were sampled in a meadow of *C. nodosa* invaded by the invasive *C. cylindracea*  
65 and in a locality of only *C. cylindracea* located in the proximity of the seagrass meadow. For  
66 comparison, the microbial community of the ambient seawater was also characterized.

67 **Materials and methods**

68 **Sampling**

69 Sampling was performed in the Bay of Funtana, northern Adriatic Sea (45°10'39" N,  
70 13°35'42" E). Leaves and thalli were sampled in a meadow of *Cymodocea nodosa* invaded by the  
71 invasive *Caulerpa cylindracea* (mixed settlement) and in a monospecific settlement of *Caulerpa*  
72 *cylindracea* located in the proximity of the meadow at approximately monthly intervals from  
73 December 2017 to October 2018 (Table S1). Leaves and thalli were collected by diving and  
74 transported to the laboratory in containers placed on ice and filled with seawater collected at  
75 the sampling site. Upon arrival to the laboratory, *C. nodosa* leaves were cut into sections of 1 –  
76 2 cm, while *C. cylindracea* thalli were cut into 5 – 8 cm long sections. Leaves and thalli were  
77 washed three times with sterile artificial seawater (ASW) to remove loosely attached microbial  
78 cells. Ambient seawater was collected in 10 l containers by diving and transported to the laboratory  
79 where 10 – 20 l were filtered through a 20 µm net. The filtrate was further sequentially filtered  
80 through 3 µm and 0.2 µm polycarbonate membrane filters (Whatman, United Kingdom) using a  
81 peristaltic pump. Filters were briefly dried at room temperature and stored at –80 °C. Seawater  
82 samples were also collected approximately monthly from July 2017 to October 2018.

83 **DNA isolation**

84 DNA from surfaces of *C. nodosa* and *C. cylindracea* was isolated using a previously modified  
85 and adapted protocol that allows for a selective epiphytic DNA isolation (Massana et al., 1997;  
86 Korlević et al., submitted). Briefly, leaves and thalli are incubated in a lysis buffer and treated  
87 with lysozyme and proteinase K. Following the incubations, the mixture containing lysed epiphytic  
88 cells was separated from the leaves and thalli and extracted using phenol-chloroform. Finally, the  
89 extracted DNA was precipitated using isopropanol. DNA from seawater picoplankton was extracted

90 from 0.2 µm polycarbonate filters according to Massana et al. (1997) with a slight modification.  
91 Following the phenol-chloroform extraction, 1/10 of chilled 3 M sodium acetate (pH 5.2) was added.  
92 DNA was precipitated by adding 1 volume of chilled isopropanol, incubating the mixtures overnight  
93 at –20 °C and centrifuging at 20,000 × g and 4 °C for 21 min. The pellet was washed twice with  
94 500 µl of chilled 70 % ethanol and centrifuged after each washing step at 20,000 × g and 4 °C for 5  
95 min. Dried pellets were re-suspended in 50 – 100 µl of deionized water.

96 **Illumina 16S rRNA sequencing**

97 Illumina MiSeq sequencing of the V4 region of the 16S rRNA gene was performed as described  
98 previously (Korlević et al., submitted). The V4 region of the 16S rRNA gene was amplified using a  
99 two-step PCR procedure. In the first PCR, the 515F (5'-GTGYCAGCMGCCGCGTAA-3') and  
100 806R (5'-GGACTACNVGGGTWTCTAAT-3') primers from the Earth Microbiome Project (<https://earthmicrobiome.org/protocols-and-standards/16s/>) were used (Caporaso et al., 2012; Apprill et al.,  
101 2015; Parada et al., 2016). These primers contained on their 5' end a tagged sequence. Purified PCR  
102 products were sent for Illumina MiSeq sequencing at IMGM Laboratories, Martinsried, Germany.  
103 Prior to sequencing at IMGM, the second PCR amplification of the two-step PCR procedure was  
104 performed using primers targeting the tagged region incorporated in the first PCR. In addition,  
105 these primers contained adapter and sample-specific index sequences. Beside samples, a positive  
106 and negative control for each sequencing batch was sequenced. The negative control comprised  
107 PCR reactions without DNA template, while for a positive control a mock community composed  
108 of evenly mixed DNA material originating from 20 bacterial strains (ATCC MSA-1002, ATCC,  
109 USA) was used. Sequences obtained in this study have been deposited in the European Nucleotide  
110 Archive (ENA) at EMBL-EBI under accession number PRJEB37267.

112 **Sequence analysis**

113       Obtained sequences were analysed on the computer cluster Isabella (University Computing  
114   Center, University of Zagreb) using mothur (version 1.43.0) (Schloss et al., 2009) according  
115   to the MiSeq Standard Operating Procedure (MiSeq SOP; [https://mothur.org/wiki/MiSeq\\_SOP](https://mothur.org/wiki/MiSeq_SOP))  
116   (Kozich et al., 2013) and recommendations provided by the Riffomonas project to enhance data  
117   reproducibility (<http://www.riffomonas.org/>). For alignment and classification of sequences the  
118   SILVA SSU Ref NR 99 database (release 138; <http://www.arb-silva.de>) was used (Quast et al.,  
119   2013; Yilmaz et al., 2014). Pipeline data processing and visualization was done using R (version  
120   3.6.0) (R Core Team, 2019) combined with packages vegan (version 2.5-6) (Oksanen et al., 2019),  
121   tidyverse (version 1.3.0) (Wickham et al., 2019) and multiple other packages (???: Neuwirth,  
122   2014; Xie, 2014, 2015, 2019; Wilke, 2018; Xie et al., 2018; Allaire et al., 2019; Zhu, 2019). The  
123   detailed analysis procedure including the R Markdown file are available in the GitHub repository  
124   ([https://github.com/MicrobesRovinj/Korlevic\\_EpiphyticDynamics\\_FrontMicrobiol\\_2021](https://github.com/MicrobesRovinj/Korlevic_EpiphyticDynamics_FrontMicrobiol_2021)). Based  
125   on the ATCC MSA-1002 mock community included in the analysis an average sequencing error  
126   rate of 0.01 % was determined, which is in line with previously reported values for next-generation  
127   sequencing data (Kozich et al., 2013; Schloss et al., 2016). In addition, the negative controls  
128   processed together with the samples yielded on average only 2 sequences after sequence quality  
129   curation.

130 **Results**

131 Sequencing of the 16S rRNA V4 region yielded a total of 1.8 million sequences after quality  
132 curation and exclusion of sequences without known relatives (no relative sequences) and eukaryotic,  
133 chloroplast and mitochondrial sequences (Table S1). A total of 35 samples originating from  
134 epiphytic archaeal and bacterial communities associated with surfaces of the seagrass *C. nodosa*  
135 and the macroalga *C. cylindracea* were analysed. In addition, 18 samples (one of the samples was  
136 sequenced twice) originating from the ambient seawater were also processed for comparison. The  
137 number of reads per sample ranged between 8,408 and 77,463 sequences (Table S1). Even when  
138 the highest sequencing effort was applied the rarefaction curves did not level off as commonly  
139 observed in high-throughput 16S rRNA amplicon sequencing approaches (Fig. S1). Following  
140 quality curation and exclusion of sequences as mentioned above reads were clustered into 28,750  
141 different OTUs at a similarity level of 97 %. Read numbers were normalized to the minimum  
142 number of sequences (8,408, Table S1) through rarefaction resulting in 17,025 different OTUs with  
143 347 to 1,977 OTUs per sample (Fig. S2). To determine seasonal changes in richness and diversity  
144 the observed number of OTUs, Chao1, ACE, Exponential Shannon and Inverse Simpson (Jost,  
145 2006) were calculated after normalization through rarefaction. Generally, richness estimators and  
146 diversity indices showed similar trends. On average, higher values were found for *C. cylindracea*  
147 (mixed [Number of OTUs,  $1,683.5 \pm 128.5$  OTUs] and monospecific [Number of OTUs,  $1,729.9 \pm$   
148 145.8 OTUs]) than for *C. nodosa* (Number of OTUs,  $1,052.2 \pm 211.4$  OTUs) and lowest values were  
149 obtained for the microbial community of the ambient seawater (Number of OTUs,  $529.2 \pm 146.8$   
150 OTUs) (Fig. S2). Seasonal changes did not reveal such large dissimilarities. *C. nodosa* communities  
151 showed a slow increase towards the end of the study, while *C. cylindracea* (mixed and monospecific)  
152 communities were characterized by slightly higher values in spring and summer than in autumn and  
153 winter (Fig. S2).

154 To determine the proportion of shared archaeal and bacterial OTUs and communities sampled  
155 in different environments the Jaccard's Similarity Coefficient on presence-absence data and

156 Bray-Curtis Similarity Coefficient, respectively, were calculated. Coefficients were determined after  
157 normalization through rarefaction and binning of samples from the particular environment. The  
158 highest proportion of shared OTUs and community was found between mixed and monospecific *C.*  
159 *cylindracea* (Jaccard, 0.35; Bray-Curtis, 0.77), while lower shared values were calculated between  
160 ambient seawater and epiphytic communities (Fig. 1). Shared proportion between *C. nodosa* and *C.*  
161 *cylindracea* were approximately in-between the values of mixed and monospecific *C. cylindracea*.  
162 To assess seasonal changes in the proportion of shared OTUs and communities the Jaccard's and  
163 Bray-Curtis Similarity Coefficients were calculated between consecutive sampling points (Fig. 2).  
164 Both coefficients showed similar trends. Temporal proportional changes were more pronounced for  
165 ambient seawater than for *C. nodosa* and especially *C. cylindracea* associated communities (Fig. 2).  
166 In addition, only 0.4 – 1.0 % of OTUs from each surface associated community were present at  
167 all seasons. These persistent OTUs constituted a high proportion of total sequences (40.2 – 52.1  
168 %). To further disentangle the environmental and seasonal community dissimilarity a Principal  
169 Coordinates Analysis (PCoA) based on Bray-Curtis distances and OTU abundances was applied. A  
170 clear separation between ambient seawater and surface associated communities was found (Fig. 3).  
171 In addition, a separation of epiphytic bacterial and archaeal communities based on host species  
172 was detected. This separation was further supported by ANOSIM ( $R = 0.96, p < 0.001$ ). Seasonal  
173 changes of *C. nodosa* associated communities indicated a separation between spring, summer and  
174 autumn/winter samples (ANOSIM,  $R = 0.54, p < 0.01$ ). For *C. cylindracea* associated communities  
175 a separation between summer and autumn/winter/spring samples was observed that was, however,  
176 not as strong as for *C. nodosa* associated communities (ANOSIM,  $R = 0.30, p < 0.05$ ) (Fig. 3).

177 The taxonomic composition of both, macrophyte associated and ambient seawater communities  
178 was dominated by bacterial ( $99.1 \pm 2.1 \%$ ) over archaeal sequences ( $0.9 \pm 2.1 \%$ ) (Fig. 4). Higher  
179 relative abundances of chloroplast related sequences were only observed in surface associated  
180 communities, with higher values in autumn/winter ( $37.2 \pm 11.2 \%$ ) than in spring/summer  
181 ( $20.9 \pm 9.7 \%$ ) (Fig. S3). Generally, at higher taxonomic ranks (phylum-class), epiphytic and  
182 ambient seawater microbial communities were composed of similar bacterial taxa. Ambient

183 seawater communities were mainly comprised of *Actinobacteriota*, *Bacteroidota*, *Cyanobacteria*,  
184 *Alphaproteobacteria*, *Gammaproteobacteria* and *Verrucomicrobiota*. Communities associated with  
185 *C. nodosa* consisted additionally of *Planctomycetota* contributing more in summer 2018 than in  
186 other seasons. In addition, communities from mixed and monospecific *C. cylindracea* were similar  
187 and characterized by the same groups as ambient seawater and *C. nodosa* communities with the  
188 addition of *Desulfobacterota* (Fig. 4). Larger differences between environments and host species  
189 were observed at lower taxonomic ranks (Figs. 5 – 9).

190 *Cyanobacteria* related sequences comprised, on average,  $5.5 \pm 4.4\%$  of total sequences (Fig. 5).  
191 Higher proportions were found for *C. nodosa* ( $16.4 \pm 5.3\%$ ) and *C. cylindracea* mixed ( $7.7 \pm 3.9$   
192 %) and monospecific ( $7.8 \pm 2.4\%$ ) associated communities in autumn and for ambient seawater  
193 communities in winter ( $8.8 \pm 7.5\%$ ). Large taxonomic differences between surface associated  
194 and ambient seawater cyanobacterial communities were observed. Ambient seawater communities  
195 were mainly comprised of *Cyanobium* and *Synechococcus*, while surface associated communities  
196 were comprised of *Pleurocapsa* and sequences within the class *Cyanobacteriia* that could not be  
197 further classified (no relative *Cyanobacteriia*) (Fig. 5). In addition, seasonal changes in surface  
198 associated communities were observed in *Pleurocapsa* and no relative *Cyanobacteriia* comprising  
199 larger proportions in autumn and winter and *Acrophormium*, *Phormidesmis* and sequences without  
200 known relatives within the *Nodosilineaceae* (no relative *Nodosilineaceae*) in spring and summer  
201 (Fig. 5).

202 Sequences classified as *Bacteroidota* comprised, on average,  $19.2 \pm 5.5\%$  of all sequences  
203 (Fig. 6). Similarly to *Cyanobacteria*, large differences in the taxonomic composition between  
204 ambient seawater and surface associated communities were found (Fig. 6). The ambient seawater  
205 community was characterized by the NS4 and NS5 marine groups, uncultured *Cryomorphaceae*,  
206 uncultured *Flavobacteriaceae*, NS11-12 marine group, *Balneola*, uncultured *Balneolaceae* and  
207 *Formosa*. In contrast, in surface associated communities *Lewinella*, *Portibacter*, *Rubidimonas*,  
208 sequences without known relatives within the *Saprospiraceae* (no relative *Saprospiraceae*),

209 uncultured *Saprospiraceae*, (sequences without known relatives within the *Flavobacteriaceae*  
210 (no relative *Flavobacteriaceae*)and uncultured *Rhodothermaceae* were found. Some groups  
211 showed minor seasonal changes such as no relative *Flavobacteriaceae* whose sequences were  
212 more abundant from November 2017 until June 2018. In contrast, uncultured *Rhodothermaceae*  
213 showed higher proportions from June 2018 until the end of the study period. Surface associated  
214 *Bacteroidota* communities were very diverse as observed in the high proportion of taxa clustering  
215 as other *Bacteroidota* (Fig. 6).

216 On average, *Alphaproteobacteria* were in comparison to the other high rank taxa the largest  
217 taxonomic group, comprising  $29.2 \pm 12.0$  % of all sequences (Fig. 7). In accordance to the above  
218 described taxa, large differences between ambient seawater and surface associated communities  
219 were observed. Ambient seawater communities were composed mainly of the SAR11 clade,  
220 AEGEAN-169 marine group, SAR116 clade, sequences without known relatives within the  
221 *Rhodobacteraceae* (no relative *Rhodobacteraceae*), HIMB11 and the OCS116 clade, while  
222 surface associated communities were composed mainly of no relative *Rhodobacteraceae* and to  
223 a lesser degree of *Pseudoahrensia*, *Amylibacter* and sequences without known relatives within  
224 the *Alphaproteobacteria* (no relative *Alphaproteobacteria*) and *Hyphomonadaceae* (no relative  
225 *Hyphomonadaceae*). Representatives of no relative *Rhodobacteraceae* comprised on average  $40.6$   
226  $\pm 23.2$  % of all alphaproteobacterial sequences in the epiphytic community (Fig. 7). In addition,  
227 *Amylibacter* was detected mainly in *C. nodosa* from November 2017 until March 2018.

228 Sequences related to *Gammaproteobacteria* comprised on average  $18.6 \pm 3.9$  % of all  
229 sequences (Fig. 8). Similar to above mentioned taxa, large taxonomic differences between ambient  
230 seawater and surface associated communities were found. Ambient seawater communities were  
231 mainly comprised of the OM60 (NOR5) clade, *Litoricola*, *Acinetobacter* and the SAR86 clade,  
232 while epiphytic communities were mainly composed of sequences without known relatives within  
233 the *Gammaproteobacteria* (no relative *Gammaproteobacteria*) and *Granulosicoccus*. Beside  
234 these two groups specific to all three epiphytic communities, *C. nodosa* was characterized by

235 *Arenicella*, *Methylotenera* and sequences without known relatives within the *Burkholderiales* (no  
236 relative *Burkholderiales*), while *Thioploca*, *Reinekea* and sequences without known relatives within  
237 *Cellvibrionaceae* (no relative *Cellvibrionaceae*) were more specific to both mixed and monospecific  
238 *C. cylindracea*. In addition, *Arenicella* was more pronounced in November and December 2017,  
239 while no relative *Burkholderiales* and *Methylotenera* were characteristic for the period from March  
240 until May 2018. For the *C. cylindracea* specific taxa no relative *Cellvibrionaceae* and *Reinekea*  
241 showed seasonality and were characteristic for samples originating from June to October 2018.  
242 In addition, similar to *Bacteroidota*, a large proportion of the surface associated community was  
243 grouped as other *Gammaproteobacteria* indicating high diversity within this group (Fig. 8).

244 *Desulfobacterota* were specific for *C. cylindracea*. In the mixed and monospecific *C.*  
245 *cylindracea* communities the proportion of *Desulfobacterota* was  $25.7 \pm 11.2\%$  and  $24.0 \pm 4.3\%$ ,  
246 respectively (Fig. 9). In contrast, in ambient seawater and *C. nodosa* communities the contribution  
247 of *Desulfobacterota* was only  $0.1 \pm 0.08\%$  and  $1.0 \pm 0.7\%$ , respectively. In *C. cylindracea* the  
248 community consisted mainly of *Desulfatitalea*, *Desulfobulbus*, *Desulfopila*, *Desulforhopalus*,  
249 *Desulfotalea*, SEEP-SRB4, uncultured *Desulfocapsaceae* and sequences without known relatives  
250 within the *Desulfobacteraceae* (no relative *Desulfobacteraceae*), *Desulfobulbaceae* (no relative  
251 *Desulfobulbaceae*) and *Desulfocapsaceae* (no relative *Desulfocapsaceae*) (Fig. 9).

252 **Discussion**

253 Surfaces of marine macrophytes harbor biofilms consisting of diverse microbial taxa (Egan  
254 et al., 2013; Tarquinio et al., 2019). No standard protocol has been developed to study these  
255 macrophyte-associated microbes (Ugarelli et al., 2019). Different procedures for removal of microbial  
256 cells from host surfaces are described, such as host tissue shaking (Nōges et al., 2010), scraping  
257 (Uku et al., 2007), swabbing (Mancuso et al., 2016) and ultrasonication (Cai et al., 2014). All  
258 these methods result in different removal efficiencies but none was enabling a complete removal of  
259 attached microbial cells based on our experience. In the present study, we applied a removal protocol  
260 (Korlević et al., submitted) based on direct cellular lysis (Burke et al., 2009). The application of a  
261 direct lysis procedure coupled with a high sampling frequency and Illumina amplicon sequencing  
262 has enabled us to described in detail the bacterial and archaeal communities associated with the  
263 surfaces of two marine macrophytes, *C. nodosa* and *C. cylindracea*.

264 In the present study, highest richness was observed for *C. cylindracea* (mixed and monospecific)  
265 followed by *C. nodosa* and lowest richness was found in ambient seawater microbial communities.  
266 Higher richness of microbial communities associated with seagrasses than in ambient seawater  
267 was described earlier and could be attributed to a larger set of inhabitable microniches existing  
268 on macrophyte surfaces than in the ambient seawater (Ugarelli et al., 2019). The highest richness  
269 observed for *C. cylindracea* might be partly due to its contact with the sediment. The stolon of *C.*  
270 *cylindracea* is attached to the sediment surface with rhizoids and thus, the stolon and rhizoids are in  
271 a direct contact with the sediment. In addition, seasonal differences in richness observed for surface  
272 attached communities indicated a slightly higher richness in spring and summer. This pattern could  
273 be explained by a higher macrophyte growth in these two seasons than in autumn and winter (M.  
274 Najdek, personal communication; Zavodnik et al., 1998; Ruitton et al., 2005). During their main  
275 growth season in spring and summer macrophytes exhibit a more dynamic chemical interaction  
276 with the surface community probably causing an increase in the number of inhabitable microniches  
277 (Borges and Champenois, 2015; Rickert et al., 2016).

278 We observed a strong differentiation between the surface attached and ambient seawater  
279 communities at the level of OTUs, in agreement with most published studies (Burke et al., 2011b;  
280 Michelou et al., 2013; Mancuso et al., 2016; Roth-Schulze et al., 2016; Crump et al., 2018;  
281 Ugarelli et al., 2019). This indicates that marine macrophytes are a selecting factor from the pool  
282 of microbial taxa present in the ambient seawater, modifying the microbial community once the  
283 macrophyte associated microbial biofilm develops (Salaün et al., 2012; Michelou et al., 2013). In  
284 contrast, Fahimipour et al. (2017) report in a global study of *Zostera marina*, similarities between  
285 the microbial community developed on leaves and in the ambient seawater. The discrepancy  
286 between our data and the study of Fahimipour et al. (2017) could be explained by different  
287 seagrass species, methodological variations or biogeographic trends as Fahimipour et al. (2017)  
288 analysed samples from different locations throughout the northern hemisphere. It is possible  
289 that the microbial communities in ambient seawater and on leaves from the same location are  
290 differing but are still more similar to each other when compared to other sampling locations.  
291 Indeed, it was found that prokaryotic communities vary substantially between different sampling  
292 sites (Bengtsson et al., 2017). When the taxonomic composition at high ranks was analysed no  
293 such strong differentiation was noticed. Phyla and classes such as *Actinobacteriota*, *Bacteroidota*,  
294 *Cyanobacteria*, *Alphaproteobacteria*, *Gammaproteobacteria* and *Verrucomicrobiota* were found in  
295 both ambient seawater as well as macrophyte associated, in agreement with previous studies (Burke  
296 et al., 2011b; Egan et al., 2013; Michelou et al., 2013). In contrast, when low taxonomic ranks  
297 were analysed (i.e., family and genus) a strong differentiation was observed (Figs. 5 – 9). A similar  
298 differentiation at lower microbial taxonomic ranks between ambient seawater and macrophytes was  
299 described for other macrophyte species as well (Egan et al., 2013; Michelou et al., 2013; Ugarelli et  
300 al., 2019).

301 Beside differences between ambient seawater and surface associated microbial communities,  
302 it is unclear whether the prokaryotic epiphytic community is host-specific or whether there are  
303 generalist taxa characteristic to all or many macrophytes (Egan et al., 2013). Similar to previously  
304 described differences between microbial communities in the ambient seawater and on macrophytes,

305 at high taxonomic ranks no major difference between the microbial communities associated with  
306 different hosts was observed. The only high rank phylum that was differing between *C. nodosa*  
307 and *C. cylindracea* was *Desulfobacterota*, with more abundant sequences in the *C. cylindracea*  
308 associated community. As already mentioned, the rhizoids and part of the stolon are in contact  
309 with the sediment. Thus *Desulfobacterota* are probably a part of the epiphytic community that  
310 was in contact with the sediment. Similar high rank taxa found in this study were described to be  
311 specific for other species of macrophytes (Burke et al., 2011b; Lachnit et al., 2011; Mancuso et  
312 al., 2016; Bengtsson et al., 2017). In contrast to high taxonomic ranks, a substantial differentiation  
313 between host specific communities was found supporting the notion that macrophyte associated  
314 microbial communities might be host-specific. Host-specificity was also observed for other species  
315 of macroalgae and seagrasses (Lachnit et al., 2011; Roth-Schulze et al., 2016; Morrissey et al.,  
316 2019; Ugarelli et al., 2019). Taken together, at high taxonomic ranks a core set of taxa could  
317 be described that is characteristic for all or many macrophytes, while at low taxonomic ranks a  
318 community specific to host species was identified (Figs. 3 and 4) (Egan et al., 2013).

319 Seasonal changes in richness in the epiphytic community were substantial as indicated by the  
320 proportion of OTUs ( $\leq 1.0\%$ ) present at every sampling date. These persistent OTUs, however,  
321 were accounting for a high proportion of sequences ( $\geq 40.2\%$ ) (Fig. 2). A very similar proportion  
322 of persistent OTUs was reported in high-frequency sampling studies describing seasonal changes in  
323 picoplankton (Gilbert et al., 2009, 2012). In comparison to the seawater community, a lower degree  
324 of seasonal shifts was observed for the macrophyte surface associated communities. It appears that  
325 microniches at the surfaces of macrophytes are providing more stable conditions than the ambient  
326 seawater. At the level of OTUs seasonal changes of *C. nodosa* and *C. cylindracea* associated  
327 communities were identified that could be linked to the growth cycle of the seagrass and macroalgae  
328 (M. Najdek, personal communication). *C. nodosa* was characterized by a spring community  
329 during maximum seagrass proliferation, a summer community during the highest standing stock of  
330 *C. nodosa* and an autumn/winter community during the decay of seagrass biomass. In contrast, *C.*  
331 *cylindracea* started to proliferate in late spring and was characterized only by a summer community

332 during high growth rates and by an autumn/winter/spring community when the biomass was at  
333 the peak and decaying thereafter. Similar seasonal changes in the epiphytic community were also  
334 described for other macroalgae (Tujula et al., 2010; Lachnit et al., 2011). Higher seasonal stability  
335 of *C. cylindracea* surface communities than in *C. nodosa* was also observed in the higher proportion  
336 of shared communities between two consecutive sampling dates in *C. cylindracea*.

337 Chloroplast sequence abundances were higher in autumn/winter than in spring/summer. This  
338 pattern is not surprising as seagrasses harbor more algal epiphytes during autumn/winter than in  
339 spring/summer (Reyes and Sansón, 2001). Furthermore, we used an adapted DNA isolation protocol  
340 that is known to partially co-extract DNA from planktonic eukaryotes (Korlević et al., 2015).  
341 Strong seasonal fluctuations of high rank epiphytic taxa were not observed, with the exception of  
342 *Cyanobacteria*. Cyanobacterial sequences were more pronounced in November and December than  
343 in spring and summer. In the months of high cyanobacterial sequence abundances the majority of  
344 sequences from this group were classified as *Pleurocapsa*, a group known to colonized different  
345 living and non-living surfaces (Burns et al., 2004; Longford et al., 2007; Mobberley et al., 2012;  
346 Reisser et al., 2014). It is possible that during periods of low metabolic activity there is a reduced  
347 interaction and selection of the epiphytic community by the seagrass, causing leaves to become  
348 a suitable surface for non-specific colonizers (Zavodnik et al., 1998). *Pleurocapsa* was replaced  
349 in spring and summer by *Acrophormium*, *Phormidesmis* and sequences without known relatives  
350 within the *Nodosilineaceae*. A study of coastal microbial mats found also a higher proportion of  
351 *Nodosilineaceae* sequences in summer, while *Phormidesmis* sequences were at their peak in autumn  
352 (Cardoso et al., 2019). Other high rank taxa did not exhibit strong successional patterns. In every  
353 analysed group, with the exception of *Desulfobacterota*, taxa present throughout the year in similar  
354 proportions and season specific taxa could be identified (Figs. 6 and 9). Within *Bacteroidota* different  
355 groups within the family *Saprospiraceae* (e.g. *Lewinella*, *Portibacter* and *Rubidimonas*) were  
356 detected across all seasons. Members of this family are often found in association with macrophytes  
357 and it is suggested that they are involved in the hydrolysis and utilization of complex carbon sources  
358 (Burke et al., 2011b; McIlroy and Nielsen, 2014; Crump et al., 2018). In contrast, the families

359 *Flavobacteriaceae* and *Rhodothermaceae* showed seasonal patterns, with *Flavobacteriaceae* being  
360 more pronounced from November to June and *Rhodothermaceae* from June to October (Fig. 6).  
361 Within *Alphaproteobacteria* the family *Rhodobacteraceae* comprised the majority of sequences  
362 throughout the year (Fig. 7). This metabolically versatile family is often associated with macrophyte  
363 surfaces and usually is one of the most abundant groups (Burke et al., 2011b; Michelou et al.,  
364 2013; Pujalte et al., 2014; Mancuso et al., 2016). In addition, *Hyphomonadaceae* were found  
365 in all samples. Interestingly, some of the species within this group contain stalks on their cells,  
366 which can be used to attach to the macrophyte surface (Weidner et al., 2000; Abraham and Rohde,  
367 2014). Within the *Gammaproteobacteria*, sequences without known representatives were the most  
368 pronounced group present throughout the year (Fig. 8). In addition, *Granulosicoccus* was also  
369 found in almost all samples. *Gammaproteobacteria* are often a major constituent of macrophyte  
370 epiphytic communities (Burke et al., 2011b; Michelou et al., 2013; Crump et al., 2018). Beside these  
371 two groups, other less abundant, taxa showed seasonal and host-specific patterns. For example, *C.*  
372 *cylindracea* harbored *Thioploca*, a known sulfur sediment bacteria and *Cellvibrionaceae*, a family  
373 with cultured members known as polysaccharide degraders (Jørgensen and Gallardo, 1999; Xie et  
374 al., 2017). *Desulfobacterota* were found only associated with *C. cylindracea* and no group within  
375 this phylum showed seasonal patterns (Fig. 9). The presence of this phylum only on *C. cylindracea*  
376 is to be expected as part of the epiphytic community is in direct contact with the sediment. The  
377 *Desulfobacterota* community was dominated by *Desulfatitalea* and no relative *Desulfocapsaceae*,  
378 known sulphate sediment groups (Kuever, 2014; Higashioka et al., 2015).

379 In temperate zones, marine macrophytes are exhibiting growth cycles, so it is not surprising that  
380 the associated epiphytic microbial community is undergoing partial seasonal changes. In the present  
381 study, we could identify in every analysed high rank taxa phylogenetic groups present throughout  
382 the year, comprising most of the sequences and a lower proportion of taxa showing seasonal  
383 patterns connected to the macrophyte growth cycle (Figs. 4 and 9). Studies focusing on functional  
384 comparisons between communities associated with different hosts showed that the majority of  
385 functions could be found in every community, indicating functional redundancy (Roth-Schulze et

386 al., 2016). This difference between phylogenetic variability and functional stability was explained  
387 by the lottery hypothesis assuming an initial random colonization step performed by a set of  
388 functionally equivalent taxonomic groups (Burke et al., 2011a; Roth-Schulze et al., 2016). It is  
389 possible that functional redundancy is a characteristic of high abundance taxa detected to be present  
390 throughout the year, while seasonal and/or host-specific functions are an attribute of taxa displaying  
391 successional patterns. Further studies connecting taxonomy with functional properties will be  
392 required to elucidate the degree of functional redundancy or specificity in epiphytic microbial  
393 communities.

## 394 **Acknowledgments**

395 This work was founded by the Croatian Science Foundation through the MICRO-SEAGRASS  
396 project (project number IP-2016-06-7118). ZZ and GJH were supported by the Austrian Science  
397 Fund (FWF) project ARTEMIS (project number P28781-B21). We would like to thank Margareta  
398 Buterer for technical support, Paolo Paliaga for help during sampling and the University Computing  
399 Center of the University of Zagreb for access to the computer cluster Isabella.

400 **References**

- 401 Abraham, W. R., and Rohde, M. (2014). “The family *Hyphomonadaceae*,” in *The*  
402 *Prokaryotes: Alphaproteobacteria and Betaproteobacteria*, eds. E. Rosenberg, E. F. DeLong,  
403 S. Lory, E. Stackebrandt, and F. Thompson (Berlin, Heidelberg: Springer-Verlag), 283–299.  
404 doi:10.1007/978-3-642-30197-1\_260.
- 405 Allaire, J. J., Xie, Y., McPherson, J., Luraschi, J., Ushey, K., Atkins, A., et al. (2019).  
406 *rmarkdown: Dynamic documents for R*.
- 407 Apprill, A., McNally, S., Parsons, R., and Weber, L. (2015). Minor revision to V4 region SSU  
408 rRNA 806R gene primer greatly increases detection of SAR11 bacterioplankton. *Aquat. Microb.*  
409 *Ecol.* 75, 129–137. doi:10.3354/ame01753.
- 410 Armstrong, E., Rogerson, A., and Leftley, J. (2000). The abundance of heterotrophic  
411 protists associated with intertidal seaweeds. *Estuar. Coast. Shelf Sci.* 50, 415–424.  
412 doi:10.1006/ECSS.1999.0577.
- 413 Bengtsson, M. M., Bühler, A., Brauer, A., Dahlke, S., Schubert, H., and Blindow, I. (2017).  
414 Eelgrass leaf surface microbiomes are locally variable and highly correlated with epibiotic  
415 eukaryotes. *Front. Microbiol.* 8, 1312. doi:10.3389/fmicb.2017.01312.
- 416 Bengtsson, M., Sjøtun, K., and Øvreås, L. (2010). Seasonal dynamics of bacterial biofilms on  
417 the kelp *Laminaria hyperborea*. *Aquat. Microb. Ecol.* 60, 71–83. doi:10.3354/ame01409.
- 418 Borges, A. V., and Champenois, W. (2015). Seasonal and spatial variability of  
419 dimethylsulfoniopropionate (DMSP) in the Mediterranean seagrass *Posidonia oceanica*. *Aquat. Bot.*  
420 125, 72–79. doi:10.1016/j.aquabot.2015.05.008.
- 421 Burke, C., Kjelleberg, S., and Thomas, T. (2009). Selective extraction of bacterial DNA from  
422 the surfaces of macroalgae. *Appl. Environ. Microbiol.* 75, 252–256. doi:10.1128/AEM.01630-08.

- 423 Burke, C., Steinberg, P., Rusch, D., Kjelleberg, S., and Thomas, T. (2011a). Bacterial  
424 community assembly based on functional genes rather than species. *Proc. Natl. Acad. Sci.*  
425 *U. S. A.* 108, 14288–14293. doi:10.1073/pnas.1101591108.
- 426 Burke, C., Thomas, T., Lewis, M., Steinberg, P., and Kjelleberg, S. (2011b). Composition,  
427 uniqueness and variability of the epiphytic bacterial community of the green alga *Ulva australis*.  
428 *ISME J.* 5, 590–600. doi:10.1038/ismej.2010.164.
- 429 Burns, B. P., Goh, F., Allen, M., and Neilan, B. A. (2004). Microbial diversity of extant  
430 stromatolites in the hypersaline marine environment of Shark Bay, Australia. *Environ. Microbiol.* 6,  
431 1096–1101. doi:10.1111/j.1462-2920.2004.00651.x.
- 432 Cai, X., Gao, G., Yang, J., Tang, X., Dai, J., Chen, D., et al. (2014). An ultrasonic method for  
433 separation of epiphytic microbes from freshwater submerged macrophytes. *J. Basic Microbiol.* 54,  
434 758–761. doi:10.1002/jobm.201300041.
- 435 Caporaso, J. G., Lauber, C. L., Walters, W. A., Berg-Lyons, D., Huntley, J., Fierer, N., et al.  
436 (2012). Ultra-high-throughput microbial community analysis on the Illumina HiSeq and MiSeq  
437 platforms. *ISME J.* 6, 1621–1624. doi:10.1038/ismej.2012.8.
- 438 Cardoso, D. C., Cretoiu, M. S., Stal, L. J., and Bolhuis, H. (2019). Seasonal development of a  
439 coastal microbial mat. *Sci. Rep.* 9, 9035. doi:10.1038/s41598-019-45490-8.
- 440 Crump, B. C., and Koch, E. W. (2008). Attached bacterial populations shared by four species  
441 of aquatic angiosperms. *Appl. Environ. Microbiol.* 74, 5948–5957. doi:10.1128/AEM.00952-08.
- 442 Crump, B. C., Wojahn, J. M., Tomas, F., and Mueller, R. S. (2018). Metatranscriptomics  
443 and amplicon sequencing reveal mutualisms in seagrass microbiomes. *Front. Microbiol.* 9, 388.  
444 doi:10.3389/fmicb.2018.00388.

445 Egan, S., Harder, T., Burke, C., Steinberg, P., Kjelleberg, S., and Thomas, T. (2013). The  
446 seaweed holobiont: Understanding seaweed-bacteria interactions. *FEMS Microbiol. Rev.* 37,  
447 462–476. doi:10.1111/1574-6976.12011.

448 Fahimipour, A. K., Kardish, M. R., Lang, J. M., Green, J. L., Eisen, J. A., and Stachowicz,  
449 J. J. (2017). Global-scale structure of the eelgrass microbiome. *Appl. Environ. Microbiol.* 83,  
450 e03391–16. doi:10.1128/AEM.03391-16.

451 Gilbert, J. A., Field, D., Swift, P., Newbold, L., Oliver, A., Smyth, T., et al. (2009). The  
452 seasonal structure of microbial communities in the Western English Channel. *Environ. Microbiol.*  
453 11, 3132–3139. doi:10.1111/j.1462-2920.2009.02017.x.

454 Gilbert, J. A., Steele, J. A., Caporaso, J. G., Steinbrück, L., Reeder, J., Temperton, B., et  
455 al. (2012). Defining seasonal marine microbial community dynamics. *ISME J.* 6, 298–308.  
456 doi:10.1038/ismej.2011.107.

457 Higashioka, Y., Kojima, H., Watanabe, T., and Fukui, M. (2015). Draft genome  
458 sequence of *Desulfatitalea tepidiphila* S28bF<sup>T</sup>. *Genome Announc.* 3, e01326–15.  
459 doi:10.1128/genomeA.01326-15.

460 Hollants, J., Leliaert, F., De Clerck, O., and Willems, A. (2013). What we can learn  
461 from sushi: A review on seaweed-bacterial associations. *FEMS Microbiol. Ecol.* 83.  
462 doi:10.1111/j.1574-6941.2012.01446.x.

463 Jost, L. (2006). Entropy and diversity. *Oikos* 113, 363–375. doi:10.1111/j.2006.0030-1299.14714.x.

464 Jørgensen, B. B., and Gallardo, V. A. (1999). *Thioploca* spp.: filamentous sulfur bacteria with  
465 nitrate vacuoles. *FEMS Microbiol. Ecol.* 28, 301–313. doi:10.1111/j.1574-6941.1999.tb00585.x.

466 Korlević, M., Markovski, M., Zhao, Z., Herndl, G. J., and Najdek, M. Selective DNA and  
467 protein isolation from marine macrophyte surfaces.

- 468 Korlević, M., Pop Ristova, P., Garić, R., Amann, R., and Orlić, S. (2015). Bacterial diversity  
469 in the South Adriatic Sea during a strong, deep winter convection year. *Appl. Environ. Microbiol.*  
470 81, 1715–1726. doi:10.1128/AEM.03410-14.
- 471 Kozich, J. J., Westcott, S. L., Baxter, N. T., Highlander, S. K., and Schloss, P. D. (2013).  
472 Development of a dual-index sequencing strategy and curation pipeline for analyzing amplicon  
473 sequence data on the MiSeq Illumina sequencing platform. *Appl. Environ. Microbiol.* 79,  
474 5112–5120. doi:10.1128/AEM.01043-13.
- 475 Kuever, J. (2014). “The family *Desulfobulbaceae*,” in *The Prokaryotes: Deltaproteobacteria*  
476 and *Epsilonproteobacteria*, eds. E. Rosenberg, E. F. DeLong, S. Lory, E. Stackebrandt, and F.  
477 Thompson (Berlin, Heidelberg: Springer-Verlag), 75–86. doi:10.1007/978-3-642-39044-9\_267.
- 478 Lachnit, T., Blümel, M., Imhoff, J. F., and Wahl, M. (2009). Specific epibacterial  
479 communities on macroalgae: Phylogeny matters more than habitat. *Aquat. Biol.* 5, 181–186.  
480 doi:10.3354/ab00149.
- 481 Lachnit, T., Meske, D., Wahl, M., Harder, T., and Schmitz, R. (2011). Epibacterial community  
482 patterns on marine macroalgae are host-specific but temporally variable. *Environ. Microbiol.* 13,  
483 655–665. doi:10.1111/j.1462-2920.2010.02371.x.
- 484 Longford, S., Tujula, N., Crocetti, G., Holmes, A., Holmström, C., Kjelleberg, S., et al. (2007).  
485 Comparisons of diversity of bacterial communities associated with three sessile marine eukaryotes.  
486 *Aquat. Microb. Ecol.* 48, 217–229. doi:10.3354/ame048217.
- 487 Mancuso, F. P., D’Hondt, S., Willems, A., Airoldi, L., and De Clerck, O. (2016). Diversity and  
488 temporal dynamics of the epiphytic bacterial communities associated with the canopy-forming  
489 seaweed *Cystoseira compressa* (Esper) Gerloff and Nizamuddin. *Front Microbiol* 7, 476.  
490 doi:10.3389/fmicb.2016.00476.

491 Margulis, L. (1991). “Symbiogenesis and symbioticism,” in *Symbiosis as a Source*  
492 of *Evolutionary Innovation: Speciation and Morphogenesis*, eds. L. Margulis and R. Fester  
493 (Cambridge, Massachusetts: The MIT Press), 1–14.

494 Massana, R., Murray, A. E., Preston, C. M., and DeLong, E. F. (1997). Vertical distribution  
495 and phylogenetic characterization of marine planktonic *Archaea* in the Santa Barbara Channel. *Appl.*  
496 *Environ. Microbiol.* 63, 50–56.

497 McIlroy, S. J., and Nielsen, P. H. (2014). “The family *Saprosiraceae*,” in *The Prokaryotes: Other Major Lineages of Bacteria and the Archaea*, eds. E. Rosenberg, E. F. DeLong, S. 498 Lory, E. Stackebrandt, and F. Thompson (Berlin, Heidelberg: Springer-Verlag), 863–889.  
499 500 doi:10.1007/978-3-642-38954-2\_138.

501 Michelou, V. K., Caporaso, J. G., Knight, R., and Palumbi, S. R. (2013). The ecology  
502 of microbial communities associated with *Macrocystis pyrifera*. *PLoS One* 8, e67480.  
503 doi:10.1371/journal.pone.0067480.

504 Miranda, L. N., Hutchison, K., Grossman, A. R., and Brawley, S. H. (2013). Diversity and  
505 abundance of the bacterial community of the red macroalga *Porphyra umbilicalis*: Did bacterial  
506 farmers produce macroalgae? *PLoS One* 8, e58269. doi:10.1371/journal.pone.0058269.

507 Mobberley, J. M., Ortega, M. C., and Foster, J. S. (2012). Comparative microbial diversity  
508 analyses of modern marine thrombolitic mats by barcoded pyrosequencing. *Environ. Microbiol.* 14,  
509 82–100. doi:10.1111/j.1462-2920.2011.02509.x.

510 Morrissey, K. L., Çavas, L., Willems, A., and De Clerck, O. (2019). Disentangling the influence  
511 of environment, host specificity and thallus differentiation on bacterial communities in siphonous  
512 green seaweeds. *Front. Microbiol.* 10, 717. doi:10.3389/fmicb.2019.00717.

513 Neuwirth, E. (2014). *RColorBrewer: ColorBrewer palettes*.

514 Nõges, T., Luup, H., and Feldmann, T. (2010). Primary production of aquatic macrophytes  
515 and their epiphytes in two shallow lakes (Peipsi and Võrtsjärv) in Estonia. *Aquat. Ecol.* 44, 83–92.  
516 doi:10.1007/s10452-009-9249-4.

517 Oksanen, J., Blanchet, F. G., Friendly, M., Kindt, R., Legendre, P., McGlinn, D., et al. (2019).  
518 *vegan: Community ecology package*.

519 Parada, A. E., Needham, D. M., and Fuhrman, J. A. (2016). Every base matters: Assessing  
520 small subunit rRNA primers for marine microbiomes with mock communities, time series and  
521 global field samples. *Environ. Microbiol.* 18, 1403–1414. doi:10.1111/1462-2920.13023.

522 Pujalte, M. J., Lucena, T., Ruvira, M. A., Arahal, D. R., and Macián, M. C. (2014). “The  
523 family *Rhodobacteraceae*,” in *The Prokaryotes: Alphaproteobacteria and Betaproteobacteria*, eds.  
524 E. Rosenberg, E. F. DeLong, S. Lory, E. Stackebrandt, and F. Thompson (Berlin, Heidelberg:  
525 Springer-Verlag), 439–512. doi:10.1007/978-3-642-30197-1\_377.

526 Quast, C., Pruesse, E., Yilmaz, P., Gerken, J., Schweer, T., Yarza, P., et al. (2013). The SILVA  
527 ribosomal RNA gene database project: Improved data processing and web-based tools. *Nucleic  
528 Acids Res.* 41, D590–D596. doi:10.1093/nar/gks1219.

529 R Core Team (2019). *R: A language and environment for statistical computing*. Vienna,  
530 Austria: R Foundation for Statistical Computing.

531 Reisser, J., Shaw, J., Hallegraeff, G., Proietti, M., Barnes, D. K. A., Thums, M., et al. (2014).  
532 Millimeter-sized marine plastics: A new pelagic habitat for microorganisms and invertebrates. *PloS  
533 One* 9, e100289. doi:10.1371/journal.pone.0100289.

534 Reyes, J., and Sansón, M. (2001). Biomass and production of the epiphytes on the leaves of  
535 *Cymodocea nodosa* in the Canary Islands. *Bot. Mar.* 44, 307–313. doi:10.1515/BOT.2001.039.

536 Rickert, E., Wahl, M., Link, H., Richter, H., and Pohnert, G. (2016). Seasonal variations in  
537 surface metabolite composition of *Fucus vesiculosus* and *Fucus serratus* from the Baltic Sea. *PLoS*  
538 *One* 11, e0168196. doi:10.1371/journal.pone.0168196.

539 Roth-Schulze, A. J., Zozaya-Valdés, E., Steinberg, P. D., and Thomas, T. (2016). Partitioning of  
540 functional and taxonomic diversity in surface-associated microbial communities. *Environ. Microbiol.*  
541 18, 4391–4402. doi:10.1111/1462-2920.13325.

542 Ruitton, S., Verlaque, M., and Boudouresque, C. F. (2005). Seasonal changes of the introduced  
543 *Caulerpa racemosa* var. *cylindracea* (Caulerpales, Chlorophyta) at the northwest limit of its  
544 Mediterranean range. *Aquat. Bot.* 82, 55–70. doi:10.1016/j.aquabot.2005.02.008.

545 Salaün, S., La Barre, S., Santos-Goncalvez, M. D., Potin, P., Haras, D., and Bazire, A.  
546 (2012). Influence of exudates of the kelp *Laminaria digitata* on biofilm formation of associated and  
547 exogenous bacterial epiphytes. *Microb. Ecol.* 64, 359–369. doi:10.1007/s00248-012-0048-4.

548 Schloss, P. D., Jenior, M. L., Koumpouras, C. C., Westcott, S. L., and Highlander, S. K. (2016).  
549 Sequencing 16S rRNA gene fragments using the PacBio SMRT DNA sequencing system. *PeerJ* 4,  
550 e1869. doi:10.7717/peerj.1869.

551 Schloss, P. D., Westcott, S. L., Ryabin, T., Hall, J. R., Hartmann, M., Hollister, E. B., et al.  
552 (2009). Introducing mothur: Open-source, platform-independent, community-supported software  
553 for describing and comparing microbial communities. *Appl. Environ. Microbiol.* 75, 7537–7541.  
554 doi:10.1128/AEM.01541-09.

555 Tarquinio, F., Hyndes, G. A., Laverock, B., Koenders, A., and Säwström, C. (2019). The  
556 seagrass holobiont: Understanding seagrass-bacteria interactions and their role in seagrass  
557 ecosystem functioning. *FEMS Microbiol. Lett.* 366, fnz057. doi:10.1093/femsle/fnz057.

- 558 Tujula, N. A., Crocetti, G. R., Burke, C., Thomas, T., Holmström, C., and Kjelleberg, S. (2010).
- 559 Variability and abundance of the epiphytic bacterial community associated with a green marine
- 560 *Ulvacean* alga. *ISME J.* 4, 301–311. doi:10.1038/ismej.2009.107.
- 561 Ugarelli, K., Laas, P., and Stingl, U. (2019). The microbial communities of leaves and roots
- 562 associated with turtle grass (*Thalassia testudinum*) and manatee grass (*Syringodium filiforme*) are
- 563 distinct from seawater and sediment communities, but are similar between species and sampling
- 564 sites. *Microorganisms* 7, 4. doi:10.3390/microorganisms7010004.
- 565 Uku, J., Björk, M., Bergman, B., and Díez, B. (2007). Characterization and comparison
- 566 of prokaryotic epiphytes associated with three East African seagrasses. *J. Phycol.* 43, 768–779.
- 567 doi:10.1111/j.1529-8817.2007.00371.x.
- 568 Weidner, S., Arnold, W., Stackebrandt, E., and Pühler, A. (2000). Phylogenetic analysis
- 569 of bacterial communities associated with leaves of the seagrass *Halophila stipulacea* by a
- 570 culture-independent small-subunit rRNA gene approach. *Microb. Ecol.* 39, 22–31.
- 571 Wickham, H., Averick, M., Bryan, J., Chang, W., McGowan, L. D., François, R., et al. (2019).
- 572 Welcome to the tidyverse. *J. Open Source Softw.* 4, 1686. doi:10.21105/joss.01686.
- 573 Wilke, C. O. (2018). *cowplot: Streamlined plot theme and plot annotations for 'ggplot2'*.
- 574 Xie, Y. (2014). “knitr: A comprehensive tool for reproducible research in R,” in *Implementing*
- 575 *Reproducible Computational Research*, eds. V. Stodden, F. Leisch, and R. D. Peng (New York:
- 576 Chapman and Hall/CRC), 3–32.
- 577 Xie, Y. (2015). *Dynamic Documents with R and knitr*. 2nd ed. Boca Raton, Florida: Chapman
- 578 and Hall/CRC.
- 579 Xie, Y. (2019). TinyTeX: A lightweight, cross-platform, and easy-to-maintain LaTeX
- 580 distribution based on TeX Live. *TUGboat* 40, 30–32.

- 581 Xie, Y., Allaire, J. J., and Golemund, G. (2018). *R Markdown: The Definitive Guide*. 1st ed.
- 582 Boca Raton, Florida: Chapman and Hall/CRC.
- 583 Xie, Z., Lin, W., and Luo, J. (2017). Comparative phenotype and genome analysis of *Cellvibrio*  
584 sp. PR1, a xylanolytic and agarolytic bacterium from the Pearl River. *BioMed Res. Int.* 2017,  
585 6304248. doi:10.1155/2017/6304248.
- 586 Yilmaz, P., Parfrey, L. W., Yarza, P., Gerken, J., Pruesse, E., Quast, C., et al. (2014). The  
587 SILVA and "All-Species Living Tree Project (LTP)" taxonomic frameworks. *Nucleic Acids Res.* 42,  
588 D643–D648. doi:10.1093/nar/gkt1209.
- 589 Zavodnik, N., Travizi, A., and de Rosa, S. (1998). Seasonal variations in the rate of  
590 photosynthetic activity and chemical composition of the seagrass *Cymodocea nodosa* (Ucr.) Asch.  
591 *Sci. Mar.* 62, 301–309. doi:10.3989/scimar.1998.62n4301.
- 592 Zhu, H. (2019). *kableExtra: Construct complex table with 'kable' and pipe syntax*.

593 **Figure legends**

594 **Fig. 1.** Proportion of shared bacterial and archaeal OTUs (Jaccard's similarity coefficient) and  
595 shared bacterial and archaeal communities (Bray-Curtis similarity coefficient) between assemblages  
596 associated with the surfaces of the macrophytes *C. nodosa* (mixed settlement) and *C. cylindracea*  
597 (mixed and monospecific settlement) and communities in the ambient seawater.

598 **Fig. 2.** Proportion of shared bacterial and archaeal communities (Bray-Curtis similarity coefficient)  
599 and shared bacterial and archaeal OTUs (Jaccard's similarity coefficient) between consecutive  
600 sampling dates and from the surfaces of the macrophytes *C. nodosa* (mixed settlement) and *C.*  
601 *cylindracea* (mixed and monospecific settlement) and in the ambient seawater.

602 **Fig. 3.** Principal Coordinates Analysis (PCoA) of Bray-Curtis distances based on OTU abundances  
603 of bacterial and archaeal communities from the surfaces of the macrophytes *C. nodosa* (mixed  
604 settlement) and *C. cylindracea* (mixed and monospecific settlement) and in the ambient seawater.  
605 Samples from the same environment or same season are labeled in different colors. The proportion  
606 of explained variation by each axis is shown on the corresponding axis in parentheses.

607 **Fig. 4.** Taxonomic classification and relative contribution of the most abundant ( $\geq 1\%$ ) bacterial  
608 and archaeal sequences on the surfaces of the macrophytes *C. nodosa* (mixed settlement) and *C.*  
609 *cylindracea* (mixed and monospecific settlement) and in the ambient seawater. NR – No Relative  
610 (sequences without known relatives within the corresponding group)

611 **Fig. 5.** Taxonomic classification and relative contribution of the most abundant ( $\geq 1\%$ )  
612 cyanobacterial sequences on the surfaces of the macrophytes *C. nodosa* (mixed settlement) and *C.*  
613 *cylindracea* (mixed and monospecific settlement) and in the ambient seawater. The proportion  
614 of cyanobacterial sequences in the total bacterial and archaeal community is given above the  
615 corresponding bar. NR – No Relative (sequences without known relatives within the corresponding  
616 group)

617 **Fig. 6.** Taxonomic classification and relative contribution of the most abundant ( $\geq 2\%$ ) sequences  
618 within the *Bacteroidota* on the surfaces of the macrophytes *C. nodosa* (mixed settlement) and *C.*  
619 *cylindracea* (mixed and monospecific settlement) and in the ambient seawater. The proportion of  
620 sequences classified as *Bacteroidota* in the total bacterial and archaeal community is given above the  
621 corresponding bar. NR – No Relative (sequences without known relatives within the corresponding  
622 group)

623 **Fig. 7.** Taxonomic classification and relative contribution of the most abundant ( $\geq 2\%$ )  
624 alphaproteobacterial sequences on the surfaces of the macrophytes *C. nodosa* (mixed settlement)  
625 and *C. cylindracea* (mixed and monospecific settlement) and in the ambient seawater. The  
626 proportion of alphaproteobacterial sequences in the total bacterial and archaeal community is given  
627 above the corresponding bar. NR – No Relative (sequences without known relatives within the  
628 corresponding group)

629 **Fig. 8.** Taxonomic classification and relative contribution of the most abundant ( $\geq 1\%$ )  
630 gammaproteobacterial sequences on the surfaces of the macrophytes *C. nodosa* (mixed settlement)  
631 and *C. cylindracea* (mixed and monospecific settlement) and in the ambient seawater. The  
632 proportion of gammaproteobacterial sequences in the total bacterial and archaeal community is  
633 given above the corresponding bar. NR – No Relative (sequences without known relatives within  
634 the corresponding group)

635 **Fig. 9.** Taxonomic classification and relative contribution of the most abundant ( $\geq 1\%$ ) sequences  
636 within the *Desulfobacterota* on the surfaces of the macrophytes *C. nodosa* (mixed settlement) and  
637 *C. cylindracea* (mixed and monospecific settlement) and in the ambient seawater. The proportion  
638 of sequences classified as *Desulfobacterota* in the total bacterial and archaeal community is given  
639 above the corresponding bar. NR – No Relative (sequences without known relatives within the  
640 corresponding group)

641 **Figures**

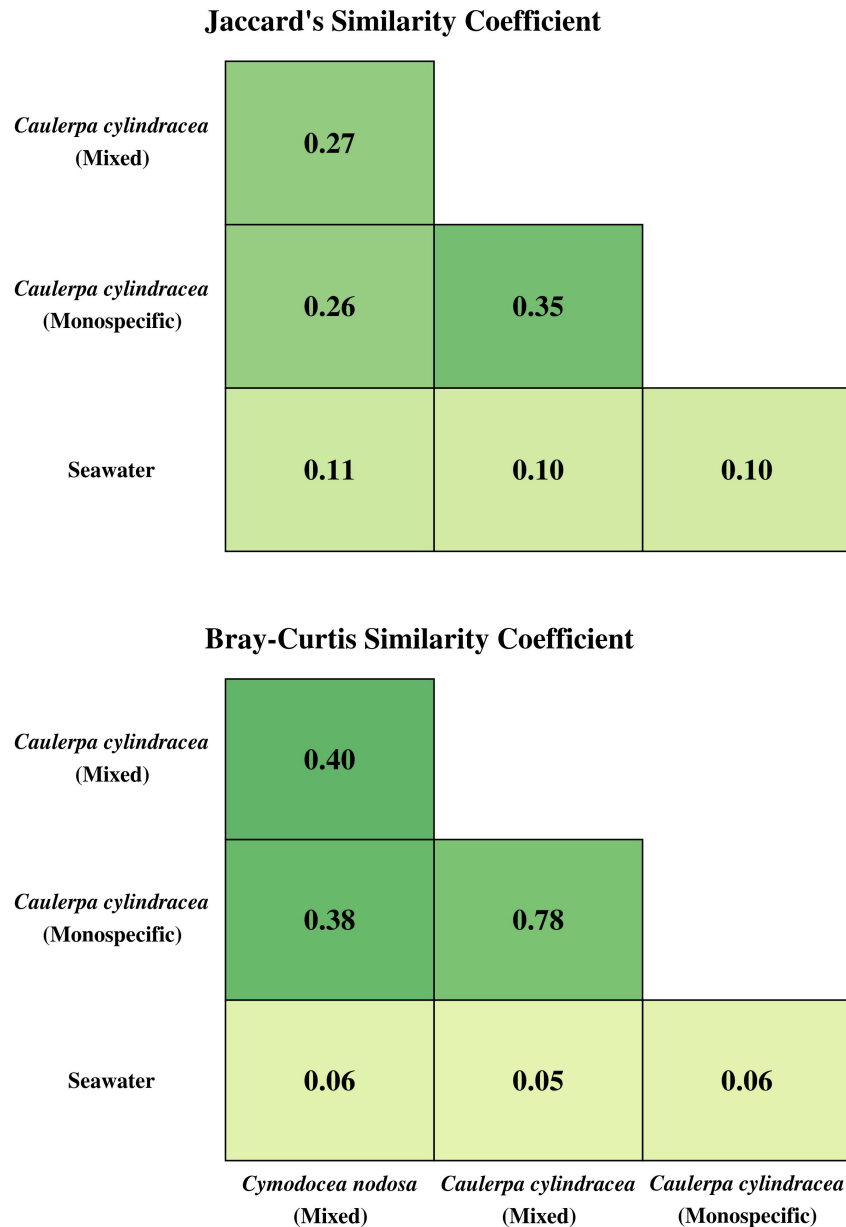


**Fig. 1.** Proportion of shared bacterial and archaeal OTUs (Jaccard's similarity coefficient) and shared bacterial and archaeal communities (Bray-Curtis similarity coefficient) between assemblages associated with the surfaces of the macrophytes *C. nodosa* (mixed settlement) and *C. cylindracea* (mixed and monospecific settlement) and communities in the ambient seawater.

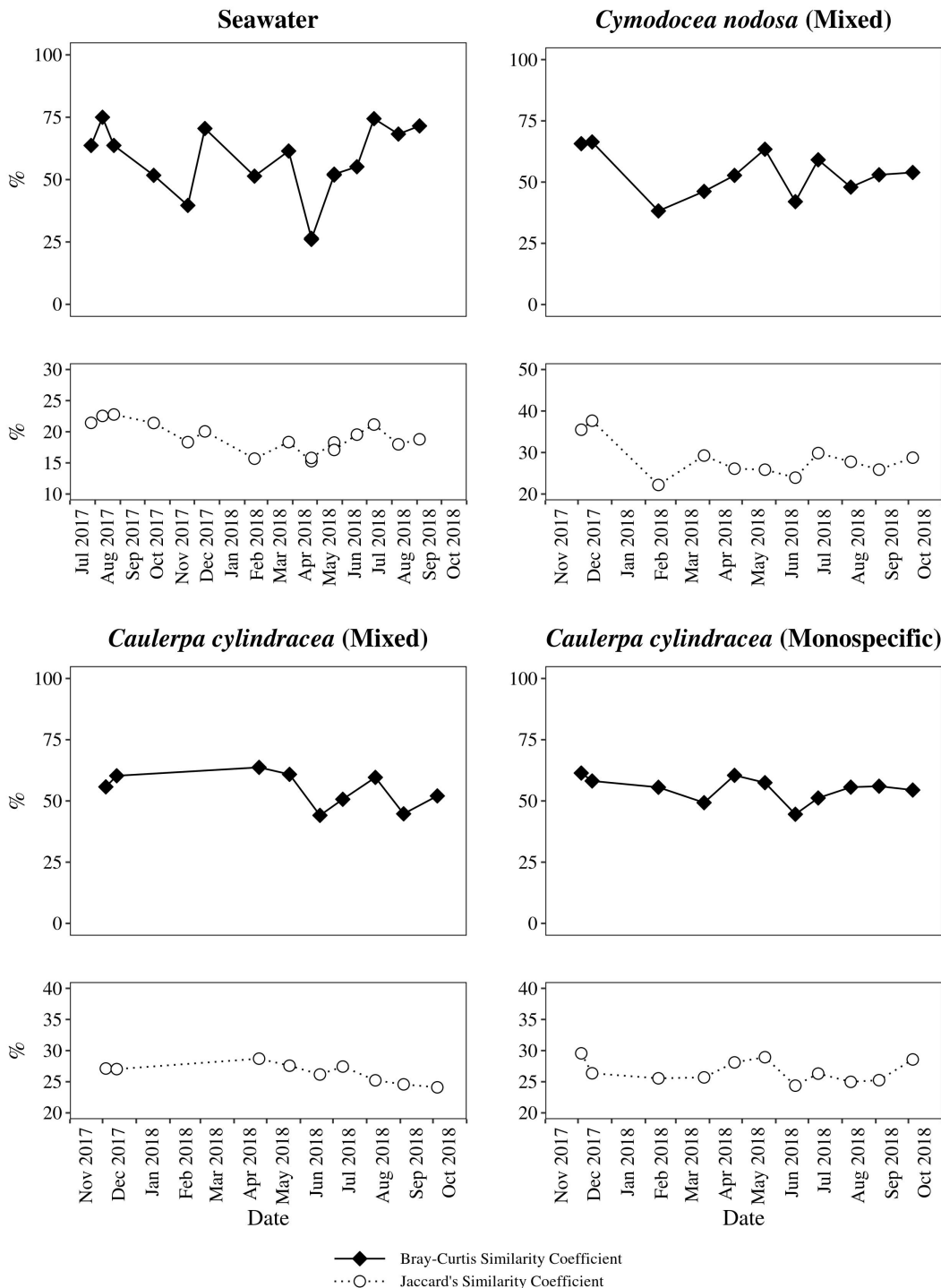


**Fig. 2.** Proportion of shared bacterial and archaeal communities (Bray-Curtis similarity coefficient) and shared bacterial and archaeal OTUs (Jaccard's similarity coefficient) between consecutive sampling dates and from the surfaces of the macrophytes *C. nodosa* (mixed settlement) and *C. cylindracea* (mixed and monospecific settlement) and in the ambient seawater.

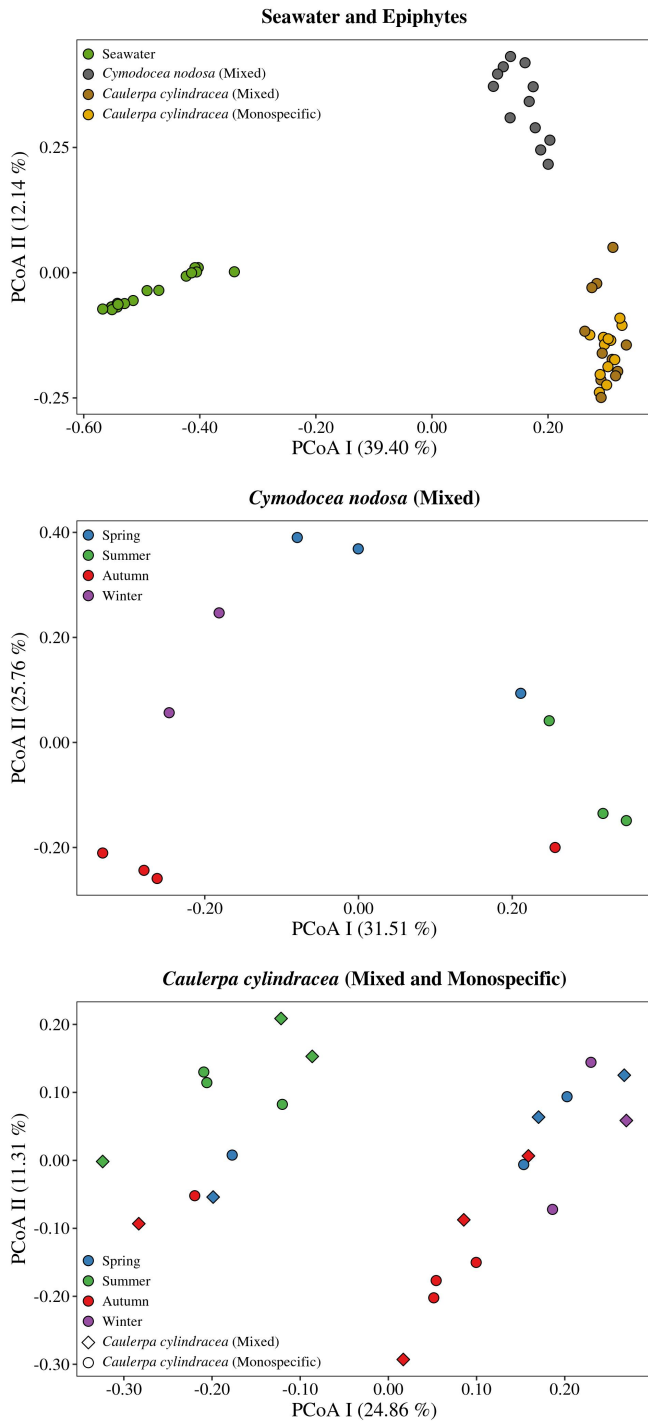


**Fig. 3.** Principal Coordinates Analysis (PCoA) of Bray-Curtis distances based on OTU abundances of bacterial and archaeal communities from the surfaces of the macrophytes *C. nodosa* (mixed settlement) and *C. cylindracea* (mixed and monospecific settlement) and in the ambient seawater. Samples from the same environment or same season are labeled in different colors. The proportion of explained variation by each axis is shown on the corresponding axis in parentheses.

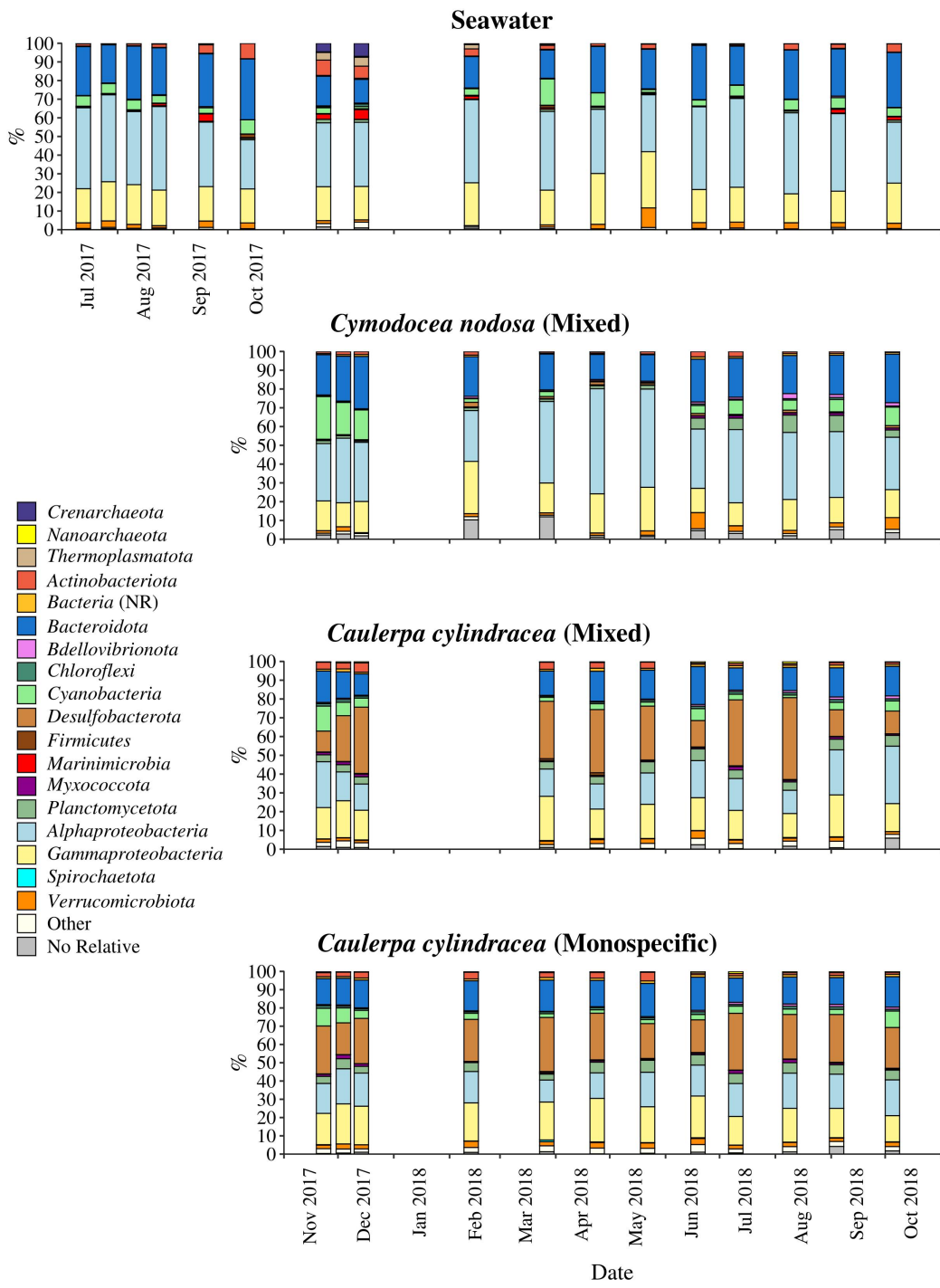


**Fig. 4.** Taxonomic classification and relative contribution of the most abundant ( $\geq 1\%$ ) bacterial and archaeal sequences on the surfaces of the macrophytes *C. nodosa* (mixed settlement) and *C. cylindracea* (mixed and monospecific settlement) and in the ambient seawater. NR – No Relative (sequences without known relatives within the corresponding group)

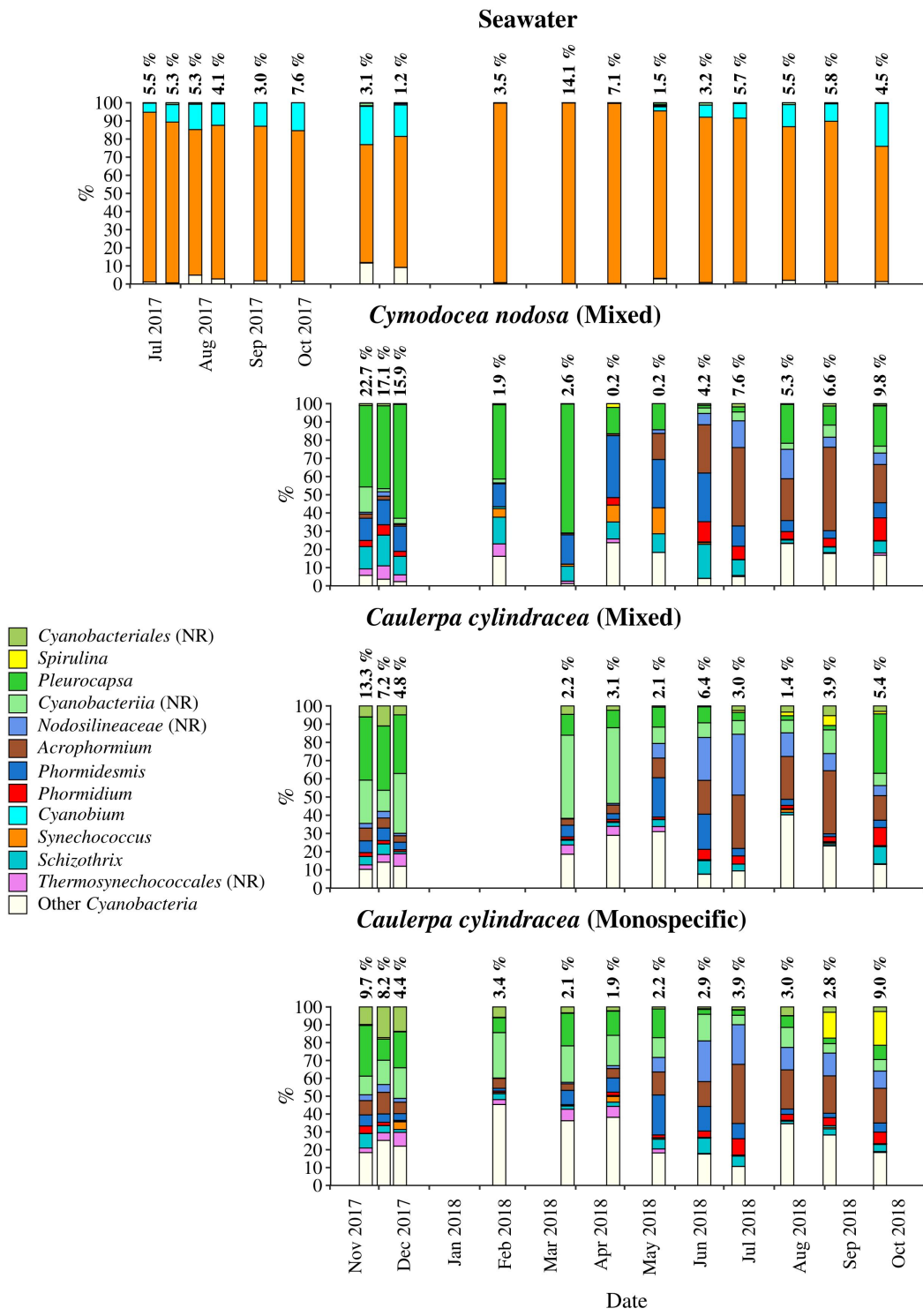


**Fig. 5.** Taxonomic classification and relative contribution of the most abundant ( $\geq 1\%$ ) cyanobacterial sequences on the surfaces of the macrophytes *C. nodosa* (mixed settlement) and *C. cylindracea* (mixed and monospecific settlement) and in the ambient seawater. The proportion of cyanobacterial sequences in the total bacterial and archaeal community is given above the corresponding bar. NR – No Relative (sequences without known relatives within the corresponding group)

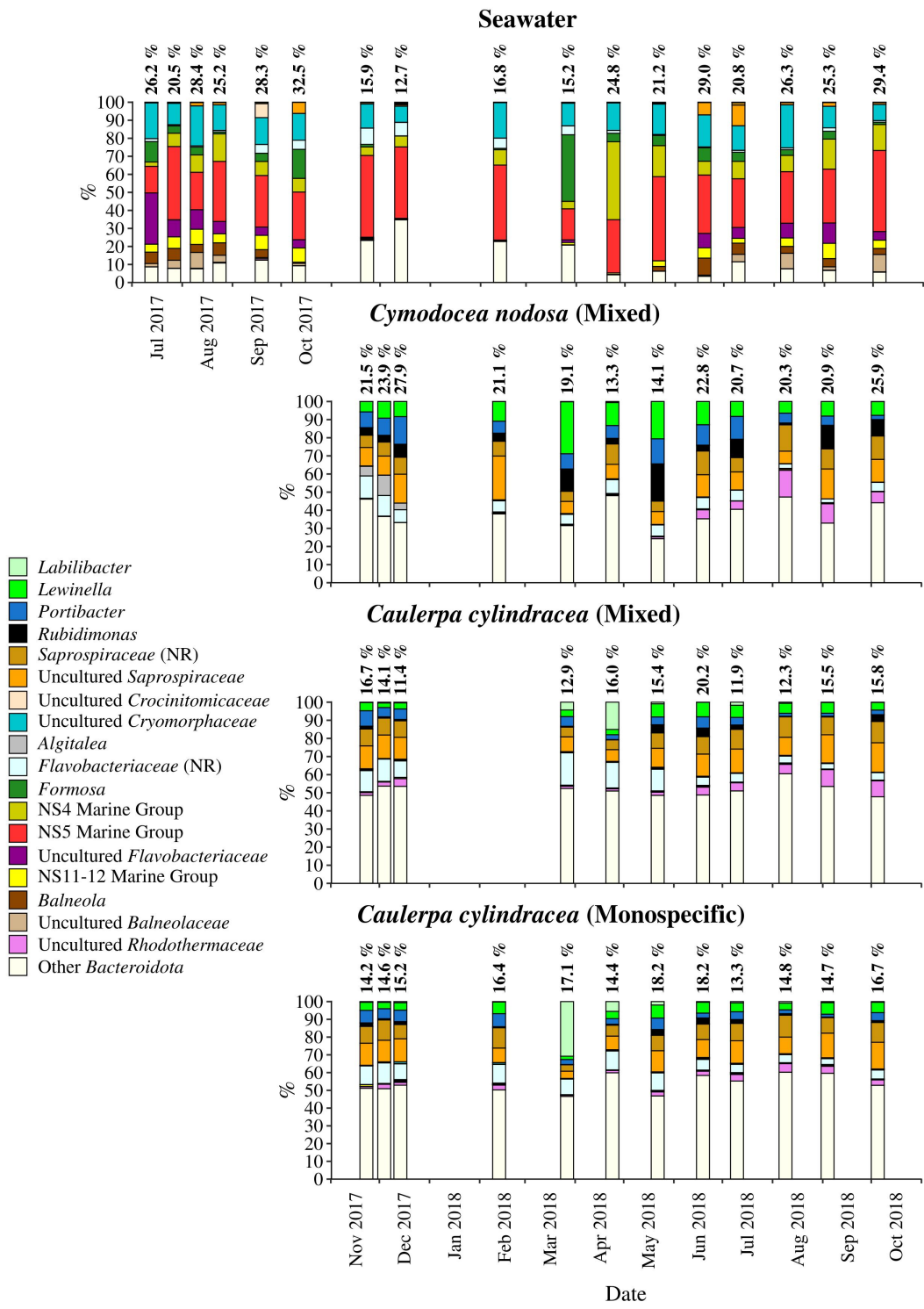


**Fig. 6.** Taxonomic classification and relative contribution of the most abundant ( $\geq 2\%$ ) sequences within the *Bacteroidota* on the surfaces of the macrophytes *C. nodosa* (mixed settlement) and *C. cylindracea* (mixed and monospecific settlement) and in the ambient seawater. The proportion of sequences classified as *Bacteroidota* in the total bacterial and archaeal community is given above the corresponding bar. NR – No Relative (sequences without known relatives within the corresponding group)

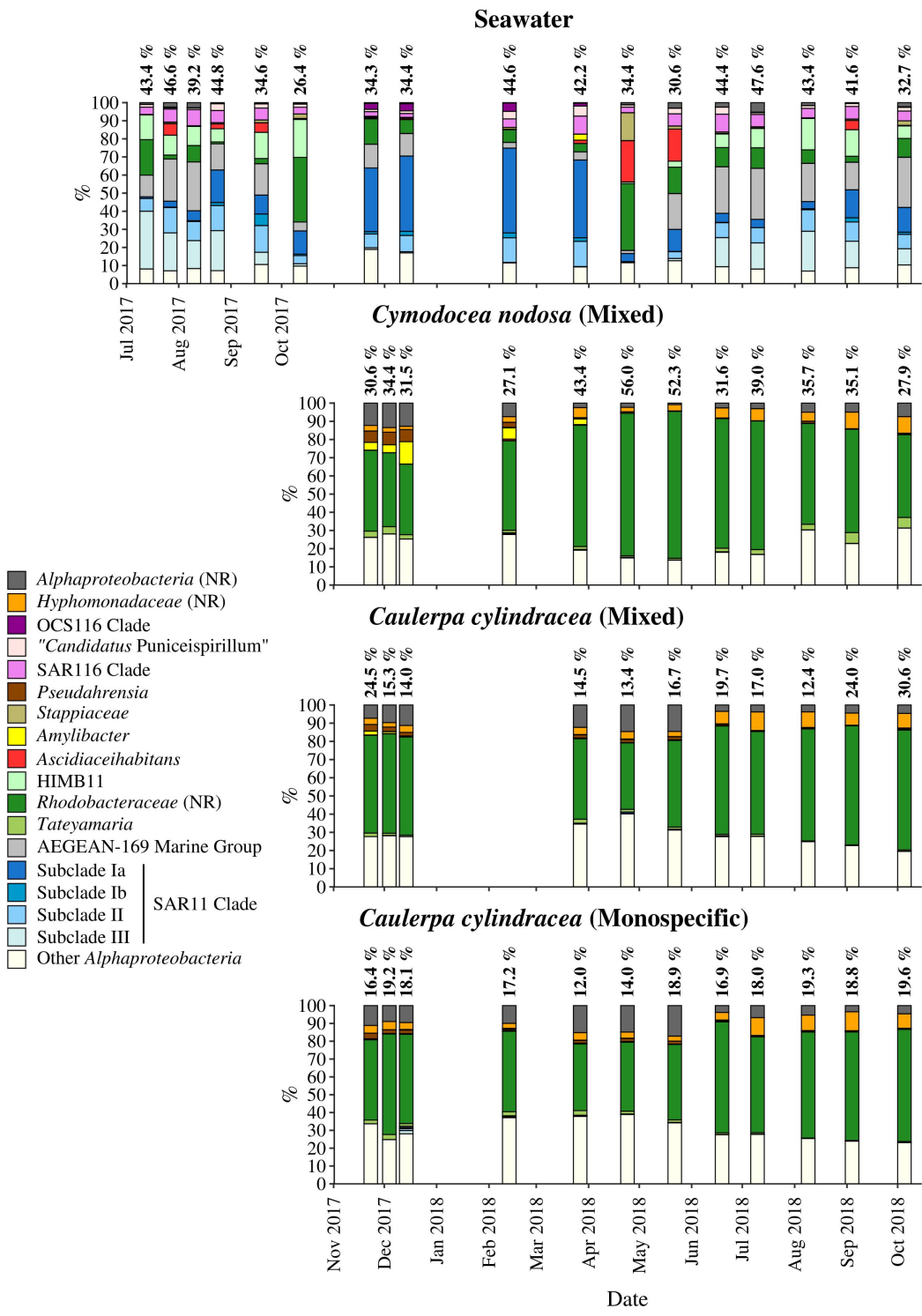


**Fig. 7.** Taxonomic classification and relative contribution of the most abundant ( $\geq 2\%$ ) alphaproteobacterial sequences on the surfaces of the macrophytes *C. nodosa* (mixed settlement) and *C. cylindracea* (mixed and monospecific settlement) and in the ambient seawater. The proportion of alphaproteobacterial sequences in the total bacterial and archaeal community is given above the corresponding bar. NR – No Relative (sequences without known relatives within the corresponding group)

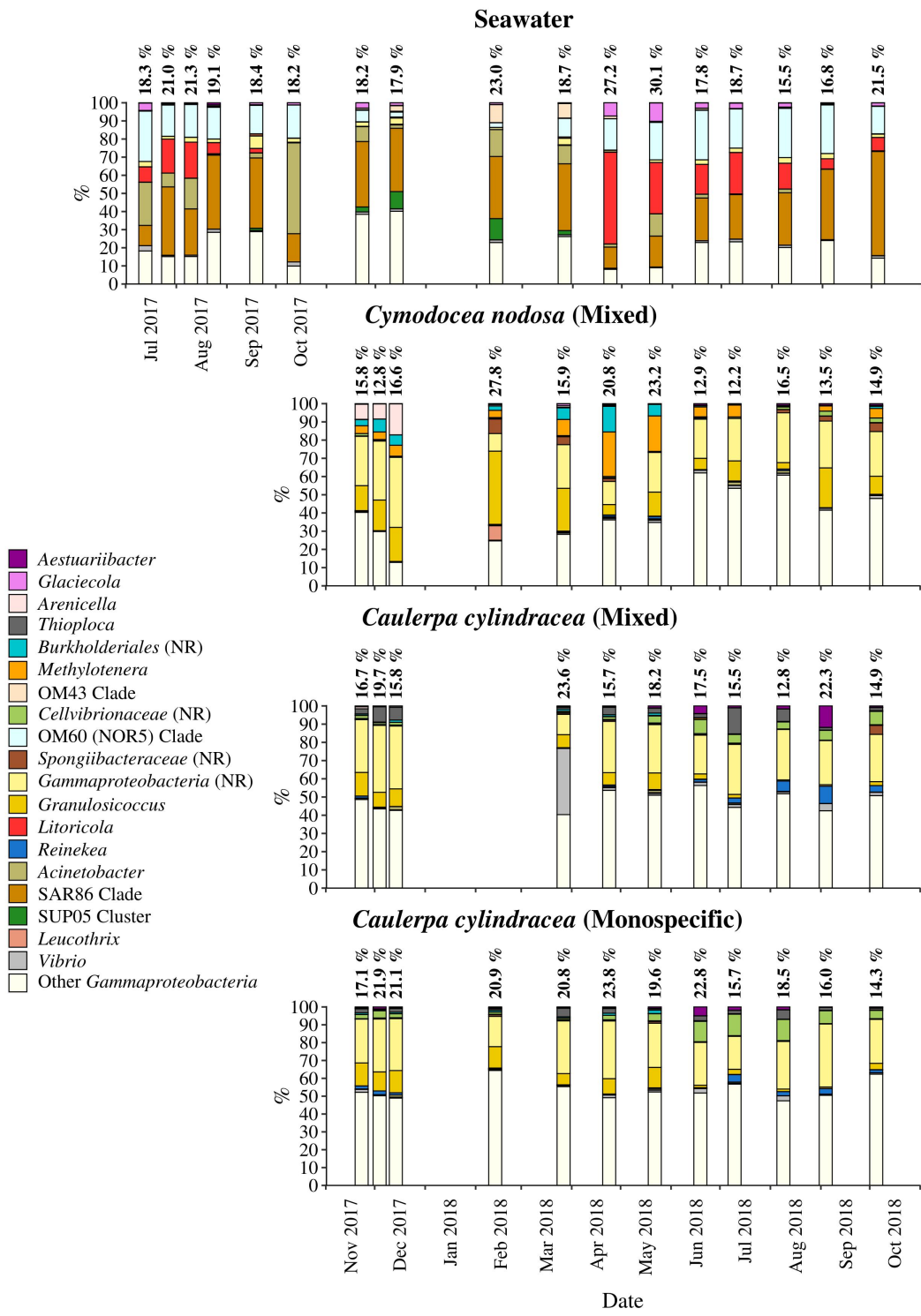


**Fig. 8.** Taxonomic classification and relative contribution of the most abundant ( $\geq 1\%$ ) gammaproteobacterial sequences on the surfaces of the macrophytes *C. nodosa* (mixed settlement) and *C. cylindracea* (mixed and monospecific settlement) and in the ambient seawater. The proportion of gammaproteobacterial sequences in the total bacterial and archaeal community is given above the corresponding bar. NR – No Relative (sequences without known relatives within the corresponding group)

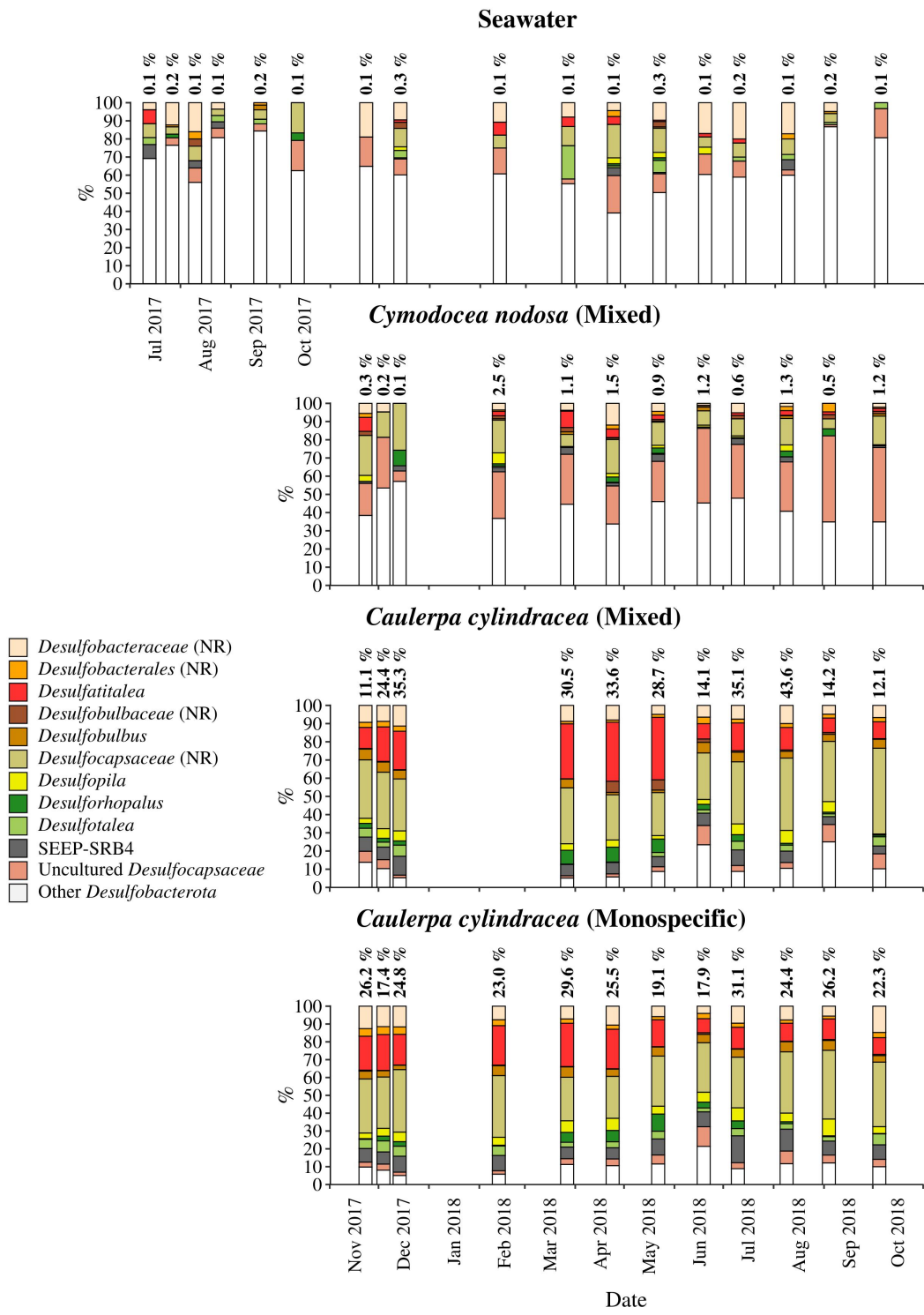


**Fig. 9.** Taxonomic classification and relative contribution of the most abundant ( $\geq 1\%$ ) sequences within the *Desulfobacterota* on the surfaces of the macrophytes *C. nodosa* (mixed settlement) and *C. cylindracea* (mixed and monospecific settlement) and in the ambient seawater. The proportion of sequences classified as *Desulfobacterota* in the total bacterial and archaeal community is given above the corresponding bar. NR – No Relative (sequences without known relatives within the corresponding group)